

Engineering superpositions of displaced number states of a trapped ion

Marcelo A. Marchioli*
*Instituto de Física de São Carlos,
Universidade de São Paulo,
Caixa Postal 369, 13560-970 São Carlos, SP, Brazil,
E-mail address: marcelo_march@bol.com.br*

Wagner Duarte José
*Universidade Estadual de Santa Cruz,
Departamento de Ciências Exatas e Tecnológicas,
Rodovia Ilhéus/Itabuna Km 16,
45650-000 Ilhéus, Bahia, Brazil,
E-mail address: wjose@uesc.br
(Dated: December 26, 2018)*

We present a protocol that permits the generation of a subtle superposition with $2^{\ell+1}$ displaced number states on a circle in phase space as target state for the center-of-mass motion of a trapped ion. Through a sequence of ℓ cycles involving the application of laser pulses and no-fluorescence measurements, explicit expressions for the total duration of laser pulses employed in the sequence and probability of getting the ion in the upper electronic state during the ℓ cycles are obtained and analyzed in detail. Furthermore, assuming that the effective relaxation process of a trapped ion can be described in the framework of the standard master equation for the damped harmonic oscillator, we investigate the degradation of the quantum interference effects inherent to superpositions via Wigner function.

I. INTRODUCTION

In quantum mechanics, the nomenclature ‘nonclassical states’ has been employed by theoretical physics for approximately seventy five years in order to designate the states of quantum systems whose statistical properties present genuine quantum effects (e.g., photon antibunching, sub-Poissonian statistics, squeezing, and quantum interference effects inherent to superposition states) without having analogous effects in classical mechanics [1]. During this period, different experimental techniques have been developed for generating and detecting both trapped and travelling nonclassical states, and more recently the nonclassical electronic and vibrational states of trapped ions. For instance, the density matrices and Wigner functions associated to the Fock states, thermal states, coherent states, squeezed vacuum states, and Schrödinger cat states (entangled position and spin superposition states), were reconstructed in laboratory through a beautiful experiment involving the quantum states of motion (motional states) of a harmonically bound ${}^9\text{Be}^+$ ion [2–5]. After this experiment, a considerable number of papers dedicated to generation and detection of nonclassical motional states have appeared in the literature [6–19]. In particular, Matos Filho and Vogel [6] have considered a class of nonlinear coherent states (NCS) which exhibits interesting nonclassical features such as strong squeezing and self-splitting with pronounced quantum interference effects, and showed that they may appear as stationary states (also recognized by the authors as dark states) of the center-of-mass (CM) motion of a trapped and bichromatically laser-driven ion far from the Lamb-Dicke regime. Man’ko et al. [12] have extended the results obtained by Matos Filho and Vogel for NCS on a circle, where the influence of nonlinear effects on the Wigner functions was discussed in detail. Furthermore, Kis et al. [14] have introduced a method by which any pure state of the quantum harmonic oscillator can be represented in a limiting sense as a NCS, and showed through a physical example how to prepare a highly excited Fock state in an ion trap based on the concept of NCS. On the other hand, Moya-Cessa et al. [10] have shown how an arbitrary superposition of coherent states can be created on a line in phase space for the motion of a single trapped ion. Pursuing this line, Duarte José and Mizrahi [11] have proposed three schemes to engineer circular states (superposition of N coherent states on a circle in phase space) for the CM motion of a

* Corresponding author: Avenida General Osório 414-centro, 14870-100 Jaboticabal, SP, Brazil.

trapped ion, where the total duration of laser pulses and the probability of getting the ion in the upper electronic state were determined for each process. In addition, the authors also have shown how the interference effects between the components of the subtle superposition can produce the Fock states.

Recently, many authors have investigated different sources of decoherence in experiments involving trapped ions and predicted interesting results which permit us to give reasonable explanations on the phenomenological decay rate of Rabi oscillations [20–23]. In this sense, Schneider and Milburn [20] have considered as decoherence source the intensity and phase fluctuations in the exciting laser pulses, and showed that a simple master equation description can be obtained since the stochastic processes involved are white noise processes. Serra et al. [21] have examined, through the analogy with the physics of surface electrons in liquid helium, the mechanism of damping and heating of trapped ions associated with the polarization of the residual background gas induced by the oscillating ions themselves. In particular, the authors have demonstrated that the decay of Rabi oscillations observed in experiments on $^9\text{Be}^+$ can be attributed to the polarization phenomena. Budini et al. [22, 23] have assumed that the origin of decoherence of the nonclassical motional states is due to the coupling of the vibronic modes with classical fields and to the finite lifetime of the electronic levels, and showed that these interactions lead to a dispersive-like decoherence dynamics. On the other hand, Poyatos et al. [24] have shown how to design different couplings (due to the absorption of a laser photon and subsequent spontaneous emission) between a single ion trapped in a harmonic potential and environment. In this scheme, the variation of the laser frequencies and intensities allows one to ‘engineer’ the coupling and select the master equation which describes the motion of the ion. Turchette et al. [25] also have presented results from an experimental study of the decoherence and decay of motional states due the interaction with several types of engineered reservoirs. Now, independently of the damping mechanisms to be considered, the degradation of the quantum interference effects in superpositions of motional states is always verified.

One of the most important applications using trapped ions was established by Cirac and Zoller [26] in the context of quantum computation, where the authors have shown that a set of N cold ions interacting with laser light and moving in a linear trap provide a realistic physical system to implement a quantum computer. The main features of this proposal are that (i) decoherence can be made negligible during the computation process, (ii) the implementation of n -bit quantum gates between any set of ions is relatively straightforward, and (iii) the quantum bit readout can be performed with efficiency approximately equal to one (a quantum bit or qubit refers to a two-state system characterized by $\{|0\rangle, |1\rangle\}$). However, the experimental realization of a quantum computer requires isolated quantum systems acting as the qubits, and the presence of controlled unitary interactions between the qubits allowing the construction of the controlled-NOT gate (basically, a controlled-NOT is defined by the operation $|\epsilon_1\rangle|\epsilon_2\rangle \rightarrow |\epsilon_1\rangle|\epsilon_1 \oplus \epsilon_2\rangle$ with \oplus denoting addition modulo 2, and $\epsilon_{1,2} = 0, 1$). Thus, if the qubits are not sufficiently isolated from the environment, different mechanisms of decoherence can destroy the quantum interferences that make the computation. The first experimental implementation of a fundamental quantum logic gate that operates on prepared quantum states in experiments involving trapped ions was realized by Monroe et al. [27]. Following the scheme proposed in [26], the authors have demonstrated a controlled-NOT gate on a pair of qubits which illustrates the basic operations necessary, and the problems associated, in the construction process of a large scale quantum computer (in this experiment, the switching speed of the controlled-NOT gate is approximately 20 kHz and the decoherence rate is of a few kHz). After the original ion-trap proposal of Cirac and Zoller, a number of modifications and extensions to their idea have appeared in the literature (e.g., see Refs. [28–33]). In summary, the investigation of noise sources in such promising quantum systems turns out to be a crucial step toward the implementation of a quantum logic processor, and consequently, of a quantum computer.

According to Kis et al. [14]: “Nonclassical states of the electromagnetic field and the atomic center-of-mass motion have played an important role in recent years, due to their relation with fundamental problems in quantum mechanics and to the many possible applications, ranging from high-resolution spectroscopy to low-noise communication and quantum computation. However, the generation of these states is usually a demanding experimental challenge.” In the present contribution, we propose a systematic scheme which permits us to engineer superpositions of displaced number states on a circle in phase space as target states for the CM motion of a trapped ion. These superpositions were studied by Marchioli et al. [34], where the authors have shown that (i) the interference effects among the state components present an analogy with diffraction patterns arising in an N slit Young-type experiment, and (ii) the interference and correlation effects are connected with the nondiagonal term of the quasiprobability distributions. In general, the superpositions of N displaced number states on a circle in phase space can be defined as follows:

$$|\Psi_n^{(N)}(\beta)\rangle \equiv N_n^{(N)} \sum_{r=1}^N \mathbf{D}(\beta_r)|n\rangle = N_n^{(N)} \sum_{r=1}^N |n, \beta_r\rangle \quad (n \in \mathbb{N}), \quad (1)$$

where $\mathbf{D}(\beta_r) = \exp(\beta_r \mathbf{a}^\dagger - \beta_r^* \mathbf{a})$ is the displacement operator with $\beta_r = |\beta| e^{i\theta_r}$ and $\theta_{r+1} - \theta_r = 2\phi$ for $\phi \in [0, 2\pi]$,

$$N_n^{(N)} = \left\{ N + 2 \sum_{r=1}^{N-1} r e^{-2|\beta|^2 \sin^2[(N-r)\phi]} \cos(|\beta|^2 \sin[2(N-r)\phi]) L_n(4|\beta|^2 \sin^2[(N-r)\phi]) \right\}^{-1/2}$$

is the normalization constant, and $L_n(z)$ is the Laguerre polynomial. An additional property of these superpositions was established in [11] for $n = 0$ and $1 \ll (e|\beta|^2/N)^N \ll 4^N$, where the interference effects approximately produce a particular Fock state; while for $(e|\beta|^2/N)^N \ll 1$, an almost vacuum state is reached. To engineer (1) we initially prepare the trapped-ion state in $|\Phi(0)\rangle = |n\rangle \otimes |\uparrow\rangle$ by means of the experimental techniques described in Refs. [2–5] (this procedure characterizes the first step of our scheme). With the help of the method established in [35] and used by Moya-Cessa et al. [10] for obtaining an arbitrary superposition of coherent states, the second step consists in the generation of superpositions of two displaced number states on a line. Now, considering the proposal of Duarte José and Mizrahi [11] for engineering circular states and adopting the motional state reached in the previous procedure as the initial motional state for this last step, we obtain, after a sequence of ℓ cycles involving the application of laser pulses and no-fluorescence measurements, the state (1) in phase space. Furthermore, the total duration T of laser pulses employed in the sequence and the probability $P_\uparrow(T)$ of getting the ion in the upper electronic state after ℓ cycles are explicitly calculated. We also verify that the quantum interference effects between the $N = 2^{\ell+1}$ components of the motional state obtained in the third step decrease the values of $P_\uparrow(T)$ when superpositions with $N \gg 1$ are regarded. Finally, assuming that the effective relaxation process of trapped ions can be described by the standard master equation for the damped harmonic oscillator [16, 25], we evaluate the time evolution of the Wigner function associated to $|\Psi_n^{(N)}(\beta)\rangle$. Following, this function is factorized into diagonal and nondiagonal terms which permits us to investigate, for example, the degradation of the undermentioned quantum interference effects through a quantitative measure of coherence introduced in [36] that characterizes the decoherence process of the nondiagonal elements of a density operator in the Fock-state basis.

This paper is organized as follows. In Section II we adopt the method proposed by Wallentowitz and Vogel [35] in order to obtain a unitary time-evolution operator which permits one to produce superpositions of two displaced number states on a line. To engineer (1) we consider in Section III the proposal of Duarte José and Mizrahi [11] for obtaining circular states, and also determine the total duration of laser pulses and the probability of getting the ion in the upper electronic state during the construction process. In Section IV we employ the Weyl-Wigner formalism to investigate the degradation of the quantum interference effects between the $2^{\ell+1}$ components of the motional state (1) through an effective relaxation process of the trapped ion. Section V contains our summary and conclusions. Finally, Appendix A describes the calculational details on the measure of coherence used in Section IV.

II. ENGINEERING SUPERPOSITIONS OF TWO DISPLACED NUMBER STATES ON A LINE

Let us consider a weak electronic transition of an ion which is bichromatically irradiated by two laser fields detuned to the first lower and first upper vibrational sidebands of the transition, respectively, with equal intensities. In the resolved-sideband and Lamb-Dicke regimes, the interaction Hamiltonian for the laser-assisted vibronic coupling can be written, in the interaction picture, as [35]

$$\mathbf{H}_{\text{int}} = \sqrt{2} \Omega (\boldsymbol{\sigma}_- e^{i\varphi} + \boldsymbol{\sigma}_+ e^{-i\varphi}) \mathbf{X}_\theta, \quad (2)$$

where $\Omega = \eta\lambda$ is the effective Rabi frequency on the first vibrational sideband with coupling constant λ and Lamb-Dicke parameter η . The electronic flip operators $\boldsymbol{\sigma}_\pm$ and $\boldsymbol{\sigma}_z$ describe the electronic transitions $|\downarrow\rangle \rightleftharpoons |\uparrow\rangle$ and satisfy the commutation relations $[\boldsymbol{\sigma}_+, \boldsymbol{\sigma}_-] = \boldsymbol{\sigma}_z$ and $[\boldsymbol{\sigma}_z, \boldsymbol{\sigma}_\pm] = \pm 2\boldsymbol{\sigma}_\pm$. The phase-rotated quadrature operator

$$\mathbf{X}_\theta \equiv \frac{\mathbf{a} e^{i\theta} + \mathbf{a}^\dagger e^{-i\theta}}{\sqrt{2}} = \mathbf{Q} \cos \theta - \mathbf{P} \sin \theta \quad (-\pi \leq \theta \leq \pi) \quad (3)$$

represents the generalized CM position of the ion, being \mathbf{a}^\dagger (\mathbf{a}) the creation (annihilation) operator of vibrational quanta. Here, the dimensionless quadrature operators \mathbf{Q} (positionlike) and \mathbf{P} (momentumlike) obey the Weyl-Heisenberg commutation relation $[\mathbf{Q}, \mathbf{P}] = i\mathbf{1}$ (for simplicity, we will fix $\hbar = 1$ throughout this paper). Furthermore, the phases $\varphi = \frac{1}{2}(\varphi_b + \varphi_r)$ and $\theta = \frac{1}{2}(\varphi_b - \varphi_r)$ contain the phases φ_b and φ_r of the lasers detuned to the blue (b) and red (r) sides of the electronic transition. In particular, when $\varphi_r = \varphi_b$ or $\varphi_r = \varphi_b + \pi$, we obtain the operators $\mathbf{X}_0 = \mathbf{Q}$ and $\mathbf{X}_{-\pi/2} = \mathbf{P}$.

Using the interaction Hamiltonian (2), we can express the unitary time-evolution operator $\mathbf{U}(t) = \exp(-it\mathbf{H}_{\text{int}})$ in a compact form as follows [10]:

$$\mathbf{U}(t) = \cos(\sqrt{2}\Omega t \mathbf{X}_\theta) - i(\boldsymbol{\sigma}_- e^{i\varphi} + \boldsymbol{\sigma}_+ e^{-i\varphi}) \sin(\sqrt{2}\Omega t \mathbf{X}_\theta). \quad (4)$$

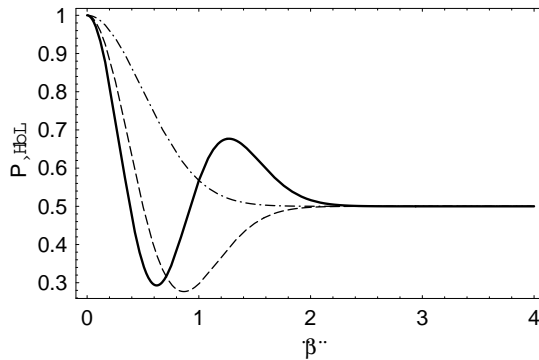


FIG. 1: Plot of $P_{\uparrow}(\beta) = \frac{1}{2}[1 + \exp(-2|\beta|^2)L_n(4|\beta|^2)]$ versus $|\beta| \in [0, 4]$ and different values of the excitation degree n , where the dot-dashed, dashed and solid lines correspond to $n = 0, 1$ and 2 , respectively.

This result allows one to determine the density operator $\rho(t) = \mathbf{U}(t)\rho(0)\mathbf{U}^\dagger(t)$ with $\rho(0) = \rho_v(0) \otimes |\uparrow\rangle\langle\uparrow|$ (being $\rho_v(0)$ the density operator for the CM motional state at time $t = 0$), and to prepare a superposition of displaced number states on a line in phase space. In fact, we are interested in generating superpositions of two displaced number states on a line using the present approach. For this purpose, the evolution operator (4) is applied on the state $|\Phi(0)\rangle = |n\rangle \otimes |\uparrow\rangle$, giving the following result:

$$|\Phi(\beta)\rangle = \frac{1}{\sqrt{2}}(|n, \beta\rangle + |n, -\beta\rangle) \otimes |\uparrow\rangle - \frac{1}{\sqrt{2}}e^{i\varphi}(|n, \beta\rangle - |n, -\beta\rangle) \otimes |\downarrow\rangle, \quad (5)$$

where $|n, \pm\beta\rangle = \mathbf{D}(\pm\beta)|n\rangle$ correspond to the displaced number states [37] and whose statistical properties were studied in detail by de Oliveira et al. [38], $\mathbf{D}(\beta) = \exp(\beta\mathbf{a}^\dagger - \beta^*\mathbf{a})$ is the displacement operator, and $\beta = i\Omega te^{-i\theta}$. The procedure of measurement of the motional state was established in [2–5], and it consists of collecting the emitted resonance fluorescence signal from the transition $|d\rangle \leftrightarrow |\downarrow\rangle$ (being $|d\rangle$ an auxiliary electronic state with width Γ on the order of $\Gamma/2\pi \approx 20$ MHz) by means of a laser strongly coupled to the electronic ground state during a specific period of time τ . Following, we consider only those events where no fluorescence have been observed, since any spontaneously emitted photon will disturb the motional quantum state via recoil effects. At this point, it is important mentioning that the efficiency in collecting the fluorescence of the trapped ion is of order of 10^{-4} (i.e., about 10^4 photons have to be scattered by the cycling electronic transition to be detected). Thus, the time needed to detect the electronic state of the ion is approximately equal to $\tau_d \approx 200\mu\text{s}$ [39, 40]. Now, if one considers the measurement time (τ_d) in the evaluation of the total time (τ_t) necessary to prepare the target state, one obtains $\tau_t \approx \tau + 200\mu\text{s}$. Consequently, the quantum state (5) is projected onto the excited state $|\uparrow\rangle$ and the resulting conditioned vibronic quantum state reads

$$|\tilde{\Phi}(\beta)\rangle = \frac{\mathcal{N}_n^{(2)}}{\sqrt{2}}(|n, \beta\rangle + |n, -\beta\rangle) \otimes |\uparrow\rangle, \quad (6)$$

being $\mathcal{N}_n^{(2)}$ the normalization factor. In particular, the probability $P_{\uparrow}(\beta)$ for the occurrence of the no-fluorescence event is connected with the normalization factor through the relation $|\mathcal{N}_n^{(2)}|^2 P_{\uparrow}(\beta) = 1/2$, and its maximum and minimum points depend on the excitation degree n of the motional state described by Eq. (6). Figure 1 shows the plot of $P_{\uparrow}(\beta)$ versus $|\beta|$ for $n = 0$ (dot-dashed line), 1 (dashed line) and 2 (solid line), where we observe that the maximum of this function reaches $P_{\uparrow} \approx 0.68$ when $n = 2$ and $|\beta| \approx 1.27$ (for instance, if one considers $\eta \approx 0.1$ and $\lambda/2\pi \approx 1$ MHz, this value of $|\beta|$ corresponds to $\tau_t \approx 202\mu\text{s}$ which is greater than $2\pi/\Gamma \approx 0.05\mu\text{s}$).

III. ENGINEERING SUPERPOSITIONS OF DISPLACED NUMBER STATES ON A CIRCLE

In this third step, we adopt the procedure established by Duarte José et al. [11, 16] which is based on a Kerr-type interaction obtained through the interaction between the trapped ion and one pair of laser beams tuned in resonance with the electronic transition frequency. In the Lamb-Dicke regime (for more details, see Refs. [41–43]), the carrier Hamiltonian of this system can be approximated as follows [11]:

$$\mathcal{H} = \Lambda\sigma_x \exp\left(-\frac{\kappa^2}{2}\right) \left[\mathbf{1} - \kappa^2\mathbf{n} + \frac{\kappa^4}{4}(\mathbf{n}^2 - \mathbf{n}) - \frac{\kappa^6}{36}(\mathbf{n}^3 - 3\mathbf{n}^2 + 2\mathbf{n}) + \dots \right] \approx \Lambda\sigma_x (\mathbf{1} - \kappa^2\mathbf{n}), \quad (7)$$

where Λ is the effective Rabi frequency, κ is the Lamb-Dicke parameter, $\mathbf{n} = \mathbf{a}^\dagger \mathbf{a}$ is the phonon-number operator, and $\mathbf{1}$ is the identity operator. It is important mentioning that the validity of the Hamiltonian \mathcal{H} essentially depends on the condition $(\kappa^2/4)\langle \mathbf{a}^\dagger \mathbf{a}^2 \rangle \ll \langle \mathbf{a}^\dagger \mathbf{a} \rangle$, i.e., this condition must be satisfied in order to guarantee the validity of the approximation employed in (7). In addition, we also consider the vibronic quantum state (6) as an initial state for the third step of the protocol.

To construct superpositions of displaced number states on a circle we have used the sequence outlined in Ref. [11] which consists of ℓ cycles involving the application of laser pulses and no-fluorescence measurements. In fact, each cycle consists in the application of one laser pulse with specific duration t_k (in order to generate the required superposition) followed by one no-fluorescence measurement (this event assures no-recoil effects of the vibrational motion of a trapped ion, and maximizes the probability to realize successfully the target state). Now, if in a particular cycle of measurements a fluorescence emission is detected, the sequence must be stopped and repeated again. Thus, after ℓ cycles of successful measurements, the resulting conditioned vibronic quantum state becomes

$$|\tilde{\Phi}(t_1 + \dots + t_\ell)\rangle = \sqrt{2} \mathcal{M}_n^{(\ell)} \left[\prod_{k=1}^{\ell} \langle \uparrow | \mathbf{U}(t_k) | \uparrow \rangle \right] (|n, \beta\rangle + |n, -\beta\rangle) \otimes | \uparrow \rangle, \quad (8)$$

where

$$\mathbf{U}(t_k) = \exp[-it_k (\Lambda \mathbf{1} - \bar{\Lambda} \mathbf{n}) \sigma_x] \quad (\bar{\Lambda} \equiv \kappa^2 \Lambda) \quad (9)$$

is the unitary time-evolution operator at time t_k associated to the carrier Hamiltonian \mathcal{H} . To engineer the ion CM motional state as Eq. (1), we need to adjust the phases in (8) of the displaced number states putting them evenly distributed around the circle: this fact is only possible when the duration of the k th evolution pulse is given by $t_k = \pi / (2^{k+1} \bar{\Lambda})$. Furthermore, we have chosen conveniently the Lamb-Dicke parameter as $\kappa^2 = (n + 2^{\ell+2})^{-1}$, which permits us to write the superposition (8) in the simplified form

$$|\tilde{\Phi}(t_1 + \dots + t_\ell)\rangle = |\Psi_n^{(2^{\ell+1})}(\beta)\rangle \otimes | \uparrow \rangle \quad (10)$$

since $\phi = \pi/2^{\ell+1}$, $\theta_r = 2\pi r/2^{\ell+1}$ with $r = 1, \dots, 2^{\ell+1}$, and $N = 2^{\ell+1}$ are fixed a priori. The final adjustment of phases involved in this process is reached when the phases φ_r and φ_b of the lasers described in the previous section satisfy the relation $\varphi_r = \varphi_b + \pi/4$. Consequently, the normalization constants $\mathcal{M}_n^{(\ell)}$ and $N_n^{(2^{\ell+1})}$ can be connected by means of the equality $\mathcal{M}_n^{(\ell)} = 2^{(\ell+1)/2} N_n^{(2^{\ell+1})}$.

The total duration $T = t_1 + \dots + t_\ell$ of laser pulses employed in the sequence, the total time T_t necessary to prepare the target states (10), and the probability $P_\uparrow(T)$ of getting the ion in the upper electronic state during the ℓ cycles, i.e.,

$$T = \frac{\pi}{2\bar{\Lambda}} (n + 2^{\ell+2}) (1 - 2^{-\ell}), \quad (11)$$

$$T_t = T + \ell\tau_d + \tau_t, \quad (12)$$

and

$$P_\uparrow(T) = \frac{1}{2^{\ell+1}} + \frac{1}{2^{2\ell+1}} \sum_{r=1}^{2^{\ell+1}-1} r \exp\left[-2|\beta|^2 \sin^2\left(\frac{\pi r}{2^{\ell+1}}\right)\right] \cos\left[|\beta|^2 \sin\left(\frac{2\pi r}{2^{\ell+1}}\right)\right] L_n\left[4|\beta|^2 \sin^2\left(\frac{\pi r}{2^{\ell+1}}\right)\right], \quad (13)$$

permit us to characterize completely the construction process. It is important mentioning that $N_n^{(2^{\ell+1})}$ and $P_\uparrow(T)$ are connected through the relation $|N_n^{(2^{\ell+1})}|^2 P_\uparrow(T) = 2^{-2(\ell+1)}$. As an application of the results obtained until the present moment we consider the engineering of superpositions with $N = 4$ and 8 displaced number states, which correspond to different sequences involving $\ell = 1$ and 2 cycles each one, and analyze their respective success through the probability (13). Figure 2 shows the plot of $P_\uparrow(T)$ versus $|\beta|$ for (a) $\ell = 1$ and (b) $\ell = 2$, with $n = 0$ (dot-dashed line), 1 (dashed line) and 2 (solid line) fixed in both situations. In Fig. 2(a) the maximum of this function reaches $P_\uparrow \approx 0.37$ (0.34) when $n = 1$ (2) and $|\beta| \approx 1.65$ (1.28), with $\kappa \approx 0.33$ (0.32) and $T_t \approx 401.93 \mu\text{s}$ (401.85 μs) if one considers $2\pi/\Lambda \approx 1 \mu\text{s}$. On the other hand, in Fig. 2(b) this maximum reaches $P_\uparrow \approx 0.25$ (0.20) for $n = 1$ (2) and $|\beta| \approx 1.96$ (3.03) with $\kappa \approx 0.24$ (0.23) and $T_t \approx 604.5 \mu\text{s}$ (605.5 μs). Furthermore, note that for $n = 2$ and $|\beta| \approx 1.27$ the probability $P_\uparrow(T)$ is approximately equal to 0.34 (0.18) when the superposition has $N = 4$ (8) states. In fact, this value depends on the number of cycles involved in the sequence and decreases when superpositions with $N \gg 1$ are regarded (compare these values with that obtained in Fig. 1). The explanation of this result is associated with the quantum interference effect between the $2^{\ell+1}$ components of the motional state $|\Psi_n^{(2^{\ell+1})}(\beta)\rangle$, i.e., high values of N lead us to obtain a large number of components interfering with each other, and this interference decreases the value of $P_\uparrow(T)$.

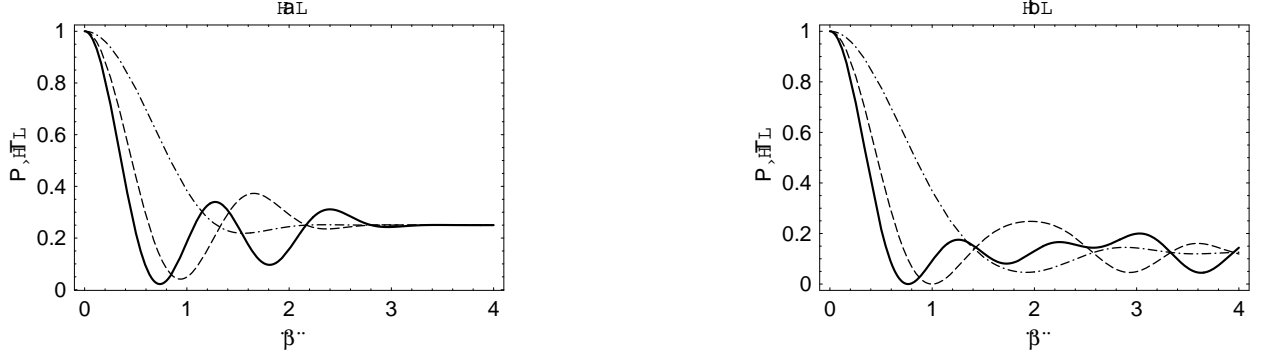


FIG. 2: Plot of $P_{\uparrow}(T)$ versus $|\beta| \in [0, 4]$ for superpositions involving (a) $N = 4$ (one cycle) and (b) $N = 8$ (two cycles) displaced number states. The total duration of laser pulses employed in both sequences for each excitation degree n is much more than that proposed by Ref. [44], where the number states were generated through a sequence of quantum nondemolition measurements on a thermal and a coherent initial state. Here, the dot-dashed, dashed and solid lines correspond to $n = 0, 1$ and 2, respectively.

IV. THE DEGRADATION OF THE QUANTUM INTERFERENCE EFFECTS VIA WIGNER FUNCTION

In this section, we adopt the procedure established by Refs. [16, 42] and assume that the effective relaxation process of trapped ions can be described in the framework of the standard master equation for the damped harmonic oscillator [45],

$$\frac{d\rho_v}{dt} = -i\omega_0 [\mathbf{a}^\dagger \mathbf{a}, \rho_v] + \gamma(\bar{n} + 1) (2\mathbf{a}\rho_v\mathbf{a}^\dagger - \mathbf{a}^\dagger\mathbf{a}\rho_v - \rho_v\mathbf{a}^\dagger\mathbf{a}) + \gamma\bar{n} (2\mathbf{a}^\dagger\rho_v\mathbf{a} - \mathbf{a}\mathbf{a}^\dagger\rho_v - \rho_v\mathbf{a}\mathbf{a}^\dagger), \quad (14)$$

where \mathbf{a} (\mathbf{a}^\dagger) is the annihilation (creation) operator associated with the oscillatory motion of frequency ω_0 in a one-dimensional harmonic trap, ρ_v describes the density operator for the CM motional state at time t , \bar{n} is the equilibrium mean number of motional quanta in the reservoir, and γ is a positive relaxation rate of the energy to thermal equilibrium (the connection between master equation and averaged interferometer approach in the trapped ion context was addressed in Ref. [25]). If one considers the Wigner representation, this equation is equivalent to the Fokker-Planck equation,

$$\frac{\partial W}{\partial t} = \left[\frac{\partial}{\partial q}(\gamma q - \omega_0 p) + \frac{\partial}{\partial p}(\gamma p + \omega_0 q) + \gamma(\bar{n} + 1/2) \left(\frac{\partial^2}{\partial q^2} + \frac{\partial^2}{\partial p^2} \right) \right] W, \quad (15)$$

for the time-dependent Wigner function $W(p, q; t)$, whose solution can be written as an integral equation [36]

$$W(p, q; t) = \int_{-\infty}^{\infty} \mathbb{K}(p, q; t|p', q'; 0) W(p', q'; 0) d\Gamma' \quad (d\Gamma' \equiv dp' dq') \quad (16)$$

with the kernel

$$\mathbb{K}(p, q; t|p', q'; 0) = [\pi(1 + 2\bar{n})u]^{-1} \exp \left\{ -[(1 + 2\bar{n})u]^{-1} \left[(p_t - e^{-\gamma t} p')^2 + (q_t - e^{-\gamma t} q')^2 \right] \right\}$$

depending on the time variable and reservoir parameters, $p_t = p \cos(\omega_0 t) + q \sin(\omega_0 t)$, $q_t = q \cos(\omega_0 t) - p \sin(\omega_0 t)$, and $u(t) = 1 - e^{-2\gamma t}$ (this function was denominated as ‘compact time’ in Refs. [16, 36]).

In order to calculate the time evolution of the Wigner function associated to the motional state $|\Psi_n^{(2^{\ell+1})}(\beta)\rangle$, firstly we substitute into the integrand of Eq. (16) the initial Wigner function [34]

$$W_n(p', q'; 0) = \frac{(-1)^n}{\pi} |N_n^{(2^{\ell+1})}|^2 \left\{ \sum_{r=1}^{2^{\ell+1}} \exp(-\Re(\mathfrak{A}_{rr})) L_n(2\Re(\mathfrak{A}_{rr})) \right. \\ \left. + 2 \sum_{s=1}^{2^{\ell+1}-1} \sum_{r=s+1}^{2^{\ell+1}} \exp[-\Re(\mathfrak{A}_{rs})] \cos[\text{Im}(\mathfrak{A}_{rs})] L_n[2\Re(\mathfrak{A}_{rs})] \right\} \quad (17)$$

with

$$\mathfrak{R}_{rs}(0) = \left[(q' + ip') - \sqrt{2} \beta_r \right] \left[(q' + ip') - \sqrt{2} \beta_s \right]^* + |\beta|^2 - \beta_r \beta_s^* .$$

Then, carrying out the integrations in the variables p' and q' , we get

$$W_n(p, q; t) = \frac{(-1)^n |\mathbb{N}_n^{(2^{\ell+1})}|^2}{\pi (1 + 2\bar{n}u)} \left[\frac{1 - 2(\bar{n} + 1)u}{1 + 2\bar{n}u} \right]^n \left\{ \sum_{r=1}^{2^{\ell+1}} \exp(-\mathfrak{F}_{rr}) L_n(2\mathfrak{G}_{rr}) \right. \\ \left. + 2 \sum_{s=1}^{2^{\ell+1}-1} \sum_{r=s+1}^{2^{\ell+1}} \operatorname{Re} [\exp(-\mathfrak{F}_{rs}) L_n(2\mathfrak{G}_{rs})] \right\} , \quad (18)$$

where

$$\operatorname{Re} [\mathfrak{F}_{rs}(t)] = \frac{\operatorname{Re} [\mathfrak{R}_{rs}(t)]}{1 + 2\bar{n}u} + \frac{2[(1 + 2\bar{n})u]|\beta|^2}{1 + 2\bar{n}u} \sin^2 \left[\frac{\pi(r-s)}{2^{\ell+1}} \right] , \\ \operatorname{Im} [\mathfrak{F}_{rs}(t)] = -\frac{\operatorname{Im} [\mathfrak{R}_{rs}(t)]}{1 + 2\bar{n}u} + \frac{[(1 + 2\bar{n})u]|\beta|^2}{1 + 2\bar{n}u} \sin \left[\frac{2\pi(r-s)}{2^{\ell+1}} \right] , \\ \operatorname{Re} [\mathfrak{G}_{rs}(t)] = \frac{(1-u)\operatorname{Re} [\mathfrak{R}_{rs}(t)]}{(1 + 2\bar{n}u)[1 - 2(\bar{n} + 1)u]} - \frac{2[(1 + 2\bar{n})u]^2|\beta|^2}{(1 + 2\bar{n}u)[1 - 2(\bar{n} + 1)u]} \sin^2 \left[\frac{\pi(r-s)}{2^{\ell+1}} \right] , \\ \operatorname{Im} [\mathfrak{G}_{rs}(t)] = \frac{[(1 + 2\bar{n})u]\operatorname{Im} [\mathfrak{R}_{rs}(t)]}{(1 + 2\bar{n}u)[1 - 2(\bar{n} + 1)u]} + \frac{(1-u)[(1 + 2\bar{n})u]|\beta|^2}{(1 + 2\bar{n}u)[1 - 2(\bar{n} + 1)u]} \sin \left[\frac{2\pi(r-s)}{2^{\ell+1}} \right] ,$$

and

$$\mathfrak{R}_{rs}(t) = \left[(q_t + ip_t) - \sqrt{2(1-u)} \beta_r \right] \left[(q_t + ip_t) - \sqrt{2(1-u)} \beta_s \right]^* + (|\beta|^2 - \beta_r \beta_s^*) (1-u) .$$

Note that $W_n(p, q; t)$ is factorized into diagonal and nondiagonal terms. This permits us, in particular, to investigate the degradation of the quantum interference effects among the $2^{\ell+1}$ components of the motional state represented by the initial Wigner function $W_n(p, q; 0)$. Similarly, Chountasis and Vourdas [46, 47] have employed the same factorization for the Weyl and Wigner functions associated with a superposition of m quantum states $|s_i\rangle$, and showed that the nondiagonal terms describe the interference effects between the states $|s_i\rangle$. To illustrate these results, in Fig. 3(a) we have plotted the three-dimensional picture of $W_n(p, q; 0)$ versus p and q (containing both diagonal and nondiagonal terms) for $n = 2$, $|\beta| = 3.03$, and $\ell = 2$ fixed; while (c) and (e) correspond to diagonal and nondiagonal terms, respectively. The influence of these terms on the shape of the Wigner function (17) leads us to confirm the results previously obtained by Chountasis and Vourdas since the nondiagonal term (e) is responsible for the interference pattern observed in (a). Now, the degradation of this pattern for $t > 0$ is connected with the effective relaxation process under consideration. To illustrate this point, we have plotted in Fig. 3(b) the three-dimensional picture of $W_n(p, q; t)$ for the same parameter set used in the previous figure, with addition of $\omega_0/\gamma = 1$, $\bar{n} = 1$ and $\gamma t = 0.1$. Furthermore, Figs. 3(d) and (f) represent the diagonal and nondiagonal terms, respectively. From the comparison between Figs. 3(a) and (b) we can perceive that the quantum interference pattern present in the first picture has disappeared in (b), and this fact is associated with the decoherence effect on the nondiagonal elements of the density operator $\rho_v(t)$ (here mapped into the nondiagonal term of $W_n(p, q; t)$ and pictured through figure 3(f)). It is important mentioning that (d) also has a significant contribution to the shape of (b), and when $\gamma t \approx 1$ this contribution is dominant if one compares with that obtained from the nondiagonal term. Similar results can be reached if $\gamma t = 0.1$ and $\bar{n} \gg 1$, since the equilibrium mean number of quanta in the reservoir represents a scale factor for the compact time $u(t)$.

The measure of coherence $\mathcal{C}(t)$ was introduced in [36] as a quantitative measurement which characterizes the rate of decoherence in the Fock-state basis. Since *decoherence* can be interpreted as the disappearance, with time progression, of the nondiagonal elements associated to the density operator $\rho_v(t)$, we will use this measure in order to explain the pattern observed in the diagonal and nondiagonal terms of $W_n(p, q; t)$. For this purpose, we define the normalized measure of coherence through the expression (for more details, see Appendix A)

$$\mathcal{C}_n^{(\ell)}(t) = \frac{\mu_n^{(\ell)}(t) - \lambda_n^{(\ell)}(t)}{\mu_n^{(\ell)}(0) - \lambda_n^{(\ell)}(0)} , \quad (19)$$

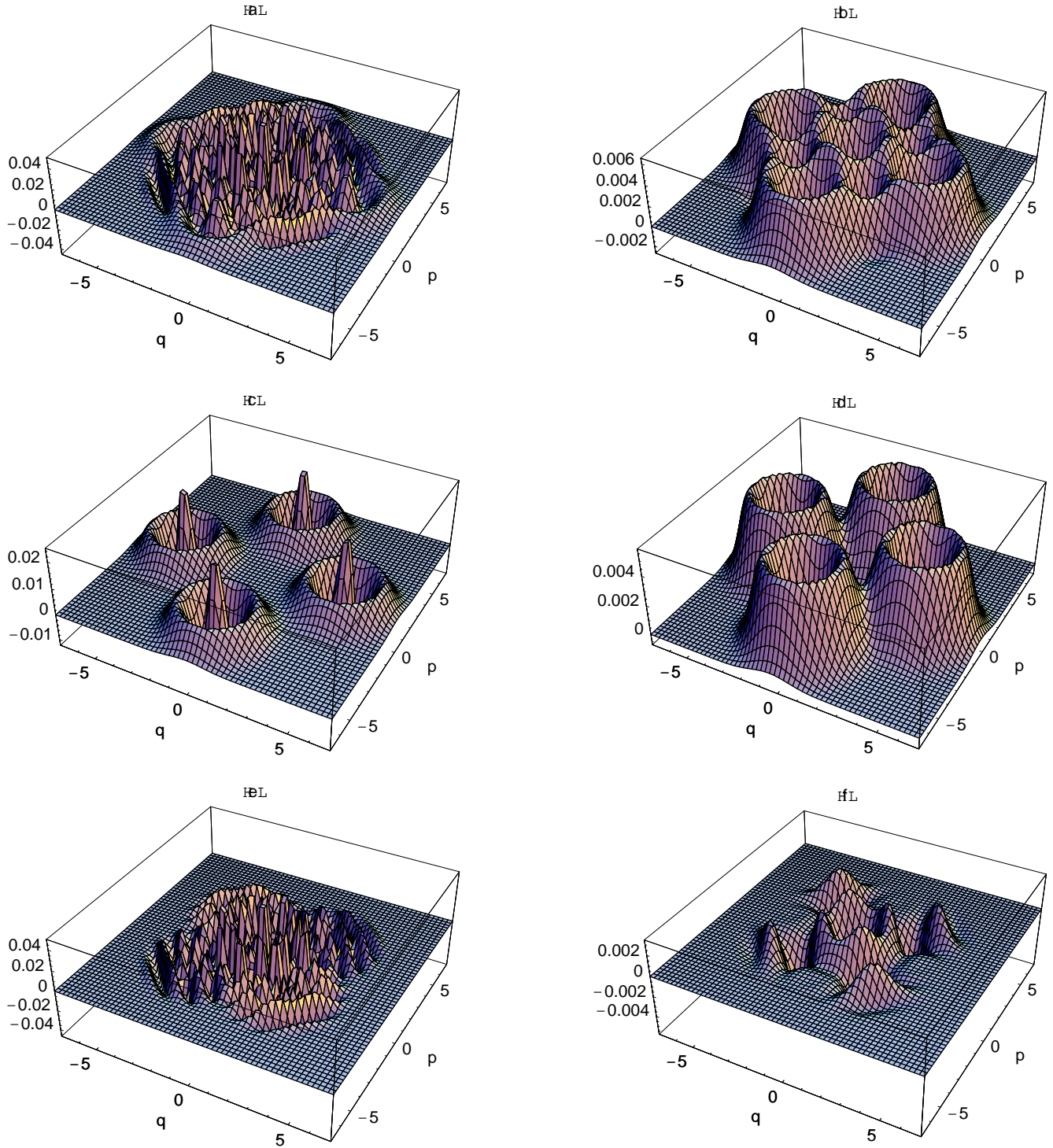


FIG. 3: The pictures (a,c,e) represent the three-dimensional plot of $W_n(p, q; 0)$ versus p and q for $n = 2$, $|\beta| = 3.03$, and $\ell = 2$; while (b,d,f) correspond to $W_n(p, q; t)$ with $\omega_0/\gamma = 1$, $\bar{n} = 1$, and $\gamma t = 0.1$. The interference pattern observed in (a) (containing both diagonal and nondiagonal terms) is a direct consequence of the nondiagonal term (e), and its disappearance in (b) is connected with the effective relaxation process under consideration.

where the ‘total purity’ $\mu_n^{(\ell)}(t)$ and ‘diagonal purity’ $\lambda_n^{(\ell)}(t)$ can be written in terms of the initial Wigner function as

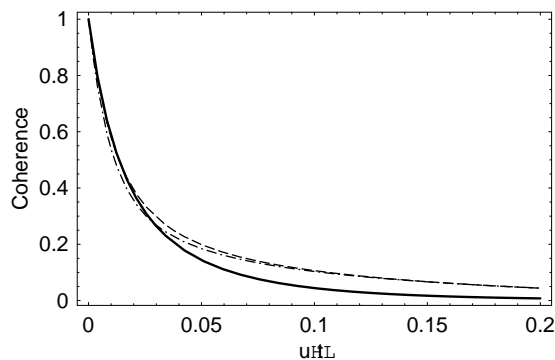


FIG. 4: Plot of $C_n^{(\ell)}(t)$ versus $u(t)$ for $|\beta| = 3.03$, $\ell = 2$, and $\bar{n} = 1$ fixed, where the dot-dashed, dashed, and solid lines correspond to $n = 0, 1$, and 2 , respectively. Note that in a short period of time ($\gamma t \in [0, 0.1116]$) and high values of ℓ and n , the measure of coherence suddenly goes to zero.

follows:

$$\mu_n^{(\ell)}(t) = \int_{-\infty}^{\infty} \int_{-\infty}^{\infty} \Xi(p', q', p'', q''; t) W_n(p', q'; 0) W_n(p'', q''; 0) d\Gamma' d\Gamma'', \quad (20)$$

$$\lambda_n^{(\ell)}(t) = \int_{-\infty}^{\infty} \int_{-\infty}^{\infty} \Delta(p', q', p'', q''; t) W_n(p', q'; 0) W_n(p'', q''; 0) d\Gamma' d\Gamma'', \quad (21)$$

being Ξ and Δ given by Eqs. (A7) and (A10), respectively. The functions $\mu_n^{(\ell)}(t)$ and $\lambda_n^{(\ell)}(t)$ were explicitly calculated in Appendix A, and their analytical results for $n = 0$ corroborate that obtained by Souza Silva et al. [16]. Figure 4 represents the plot of $C_n^{(\ell)}(t)$ versus the compact time $u(t) = 1 - e^{-2\gamma t}$ for $|\beta| = 3.03$, $\ell = 2$, and $\bar{n} = 1$ fixed, where the dot-dashed, dashed, and solid lines correspond to $n = 0, 1$, and 2 , respectively. Note that for $u = 0.2$ we obtain $C_0^{(2)} \approx 0.0443$, $C_1^{(2)} \approx 0.0438$, and $C_2^{(2)} \approx 0.0076$; while for $n = 2$, the measure of coherence goes to $C_2^{(0)} \approx 0.0428$, $C_2^{(1)} \approx 0.0247$, and $C_2^{(2)} \approx 0.0076$ at the same compact time. Otherwise, if one considers $u = 1$ in both situations, $C_n^{(\ell)}$ goes to zero for any values of ℓ and n . Thus, high values of the parameters ℓ and n considerably decrease (increase) the measure of coherence (decoherence process) in a short period of time and this fact could explain the disappearance of the quantum interference pattern observed in Fig. 3 [48].

V. SUMMARY AND CONCLUSIONS

In this paper, we have combined different theoretical approaches in order to engineer superpositions of displaced number states on a circle in phase space as target states for the center-of-mass motion of a trapped ion. The total duration T of laser pulses employed in the process and the probability $P_{\uparrow}(T)$ of getting the ion in the upper electronic state were explicitly calculated and analyzed. In particular, we have verified that (i) the quantum interference effects among the $N = 2^{\ell+1}$ components of the motional state described by Eq. (1) decrease the values of $P_{\uparrow}(T)$ when superpositions with $N \gg 1$ are regarded, and (ii) the Lamb-Dicke parameter κ essentially depends on the number ℓ of cycles involved in the sequence and the excitation degree n of the motional state. Furthermore, we have also investigated the degradation of the quantum interference effects via the Wigner function and showed that (iii) these effects basically depend on the nondiagonal term of the Wigner function at time $t = 0$, (iv) the quantum interference pattern present in $W_n(p, q; 0)$ disappears for $t > 0$ and this fact is associated with the decoherence process on the nondiagonal elements of the density operator $\rho_v(t)$, and (v) high values of the parameters ℓ and n increase the decoherence process in a short period of time. Summarizing, the work reported here is clearly the product of considerable effort and constitutes an marginally original contribution to the wider field of quantum state engineering.

Recently, Lvovsky and Babichev [49] have synthesized the displaced Fock states of the electromagnetic field by overlapping the pulsed optical single-photon Fock state with coherent states on a high-reflection beam splitter and showed its nonclassical properties (such as negativity of the Wigner function and photon number oscillations) through a complete tomographic reconstruction. However, the nonunitary quantum efficiency of the homodyne detector, the dark counts of the single-photon detector, and the impurity of the optical mode of the conditionally prepared photon represent important restrictions on the preparation and measurement of the Fock state. In this sense, experiments

involving trapped ions are a great laboratory in the construction process of nonclassical states since the decoherence time is the longest if one compares with that obtained from experiments for trapped and travelling nonclassical states of the electromagnetic field. In conclusion, we believe that the results obtained in this paper can motivate the generation of new nonclassical states in future experiments on trapped ions and to contribute significantly to the study of quantum interference effects in different physical contexts.

Acknowledgments

The author MAM acknowledges the hospitality of the *Departamento de Ciências Exatas e Tecnológicas* of *Universidade Estadual de Santa Cruz* (Ilhéus, Bahia, Brazil) where this work was initiated. WDJ acknowledges financial support from PRODOC/FAPEX, Bahia, Brazil, project no. 991042-69. MAM and WDJ are grateful to R.J. Napolitano for reading the manuscript and for providing valuable suggestions. This work was supported by FAPESP, São Paulo, Brazil, project nos. 01/11209-0 and 00/15084-5.

APPENDIX A: THE MEASURE OF COHERENCE

Dodonov et al. [36] have introduced two quantitative measures which characterize the rates of decoherence and thermalization of quantum systems, and studied the time evolution of these measures in the case of a quantum harmonic oscillator whose relaxation process is described in the framework of the standard master equation. In particular, the measure of coherence $\mathcal{C}(t)$ was defined by the authors through the expression

$$\mathcal{C}(t) = \frac{\mu(t) - \lambda(t)}{\mu(0) - \lambda(0)}, \quad (\text{A1})$$

where the functions $\mu(t) \equiv \text{Tr}[\boldsymbol{\rho}^2(t)]$ and $\lambda(t) \equiv \text{Tr}[\boldsymbol{\rho}_d^2(t)]$ ($\boldsymbol{\rho}_d(t) = \sum_{n \in \mathbb{N}} P_n(t)|n\rangle\langle n|$) correspond to the diagonal part of the density operator $\boldsymbol{\rho}(t)$, being $P_n(t) = \langle n|\boldsymbol{\rho}(t)|n\rangle$ connected with Wigner function $W(p, q; t)$ and phonon (photon) distribution function $P_n(t)$, as follow:

$$\mu(t) = \int_{-\infty}^{\infty} [W(p, q; t)]^2 d\Gamma \quad (d\Gamma = dp dq) \quad (\text{A2})$$

and

$$\lambda(t) = \sum_{n=0}^{\infty} [P_n(t)]^2. \quad (\text{A3})$$

In addition, the phonon (photon) distribution function can also be obtained by means of the auxiliary relation

$$P_n(t) = \int_{-\infty}^{\infty} W_n(p, q)W(p, q; t) d\Gamma, \quad (\text{A4})$$

being

$$W_n(p, q) = 2(-1)^n \exp[-(p^2 + q^2)] L_n[2(p^2 + q^2)]$$

the Wigner function associated to the number state at time $t = 0$. Thus, if one knows the Wigner function associated to the density operator $\boldsymbol{\rho}(t)$, then the functions ‘total purity’ $\mu(t)$ and ‘diagonal purity’ $\lambda(t)$ can be promptly calculated. Note that $\mathcal{C}(0) = 1$, and $\mathcal{C}(t) = 0$ for any completely incoherent state without nondiagonal matrix elements in the energy basis (provided that initially at least one nondiagonal element was different from zero).

Now, substituting the solution (16) of the Fokker-Planck equation for the harmonic oscillator into Eqs. (A2) and (A4), we obtain

$$\mu(t) = \int_{-\infty}^{\infty} \int_{-\infty}^{\infty} \Xi(p', q', p'', q''; t) W(p', q'; 0) W(p'', q''; 0) d\Gamma' d\Gamma'', \quad (\text{A5})$$

$$P_n(t) = \int_{-\infty}^{\infty} \mathcal{K}_n(p', q'; t) W(p', q'; 0) d\Gamma', \quad (\text{A6})$$

with

$$\Xi(p', q', p'', q''; t) = [(1 + 2\bar{n})u]^{-1} \exp \left\{ -\frac{(1-u) [(p' - p'')^2 + (q' - q'')^2]}{2(1 + 2\bar{n})u} \right\} \quad (\text{A7})$$

and

$$\begin{aligned} \mathcal{K}_n(p', q'; t) &= \frac{2(-1)^n}{1 + (1 + 2\bar{n})u} \left[\frac{1 - (1 + 2\bar{n})u}{1 + (1 + 2\bar{n})u} \right]^n \exp \left[-\frac{(1-u)(p'^2 + q'^2)}{1 + (1 + 2\bar{n})u} \right] \\ &\times L_n \left[\frac{2(1-u)(p'^2 + q'^2)}{[1 - (1 + 2\bar{n})u][1 + (1 + 2\bar{n})u]} \right]. \end{aligned} \quad (\text{A8})$$

Consequently, the function $\lambda(t)$ can also be determined through the equation

$$\lambda(t) = \int_{-\infty}^{\infty} \int_{-\infty}^{\infty} \Delta(p', q', p'', q''; t) W(p', q'; 0) W(p'', q''; 0) d\Gamma' d\Gamma'' , \quad (\text{A9})$$

where $\Delta(p', q', p'', q''; t)$ is given by

$$\begin{aligned} \Delta(p', q', p'', q''; t) &= [(1 + 2\bar{n})u]^{-1} \exp \left[-\frac{(1-u)(p'^2 + q'^2 + p''^2 + q''^2)}{2(1 + 2\bar{n})u} \right] \\ &\times I_0 \left[\frac{(1-u) [(p'^2 + q'^2)(p''^2 + q''^2)]^{1/2}}{(1 + 2\bar{n})u} \right], \end{aligned} \quad (\text{A10})$$

being $I_\nu(z)$ the modified Bessel function of the first kind [50]. This expression was obtained with the help of the intermediate relation [51]

$$\sum_{n=0}^{\infty} \frac{n! L_n^{(\nu)}(x) L_n^{(\nu)}(y)}{\Gamma(n + \nu + 1)} z^n = (1 - z)^{-1} (xyz)^{-\nu/2} \exp \left[-\frac{z(x+y)}{1-z} \right] I_\nu \left[\frac{2(xyz)^{1/2}}{1-z} \right],$$

with $|z| < 1$ and $\nu > -1$. Since the initial Wigner function does not depend on the undermentioned relaxation process, Eqs. (A5) and (A9) represent an alternative way to the calculation of the total and diagonal purities.

In many situations of practical interest both purities can be established rather easily. For instance, if one considers the initial Wigner function (17) in Eqs. (A5) and (A9), we get

$$\mu_n^{(\ell)}(t) = \frac{1}{2} \left[\frac{2|N_n^{(2\ell+1)}|^2}{n!} \right]^2 \frac{\partial^{2n}}{\partial x^n \partial y^n} \frac{(xy)^n}{xA_y + (1-u)y} \text{H}(x, y; t) \Big|_{x=y=1} \quad (\text{A11})$$

and

$$\lambda_n^{(\ell)}(t) = \left[\frac{2|N_n^{(2\ell+1)}|^2}{n!} \right]^2 \frac{\partial^{2n}}{\partial x^n \partial y^n} \frac{(xy)^n}{\mathcal{A}_+ \mathcal{B}_+ - \mathcal{A}_- \mathcal{B}_-} \text{J}(x, y; t) \Big|_{x=y=1}, \quad (\text{A12})$$

where

$$\begin{aligned} \text{H}(x, y; t) &= \sum_{p,q=1}^{2^{\ell+1}} \sum_{r,s=1}^{2^{\ell+1}} \exp \left[-2 (\mathfrak{D}_{pq}^{rs} - \mathfrak{C}_{pq}^{rs}) |\beta|^2 \right], \\ \text{J}(x, y; t) &= \sum_{p,q=1}^{2^{\ell+1}} \sum_{r,s=1}^{2^{\ell+1}} \exp \left\{ -2 \left[\frac{\mathcal{B}_+ \mathcal{A}_{rs} U_{rs} + \mathcal{A}_+ \mathcal{B}_{pq} V_{pq}}{\mathcal{A}_+ \mathcal{B}_+} + \frac{2(1-u)(\mathcal{B}_+ \mathcal{B}_- U_{rs}^2 + \mathcal{A}_+ \mathcal{A}_- V_{pq}^2)}{\mathcal{A}_+ \mathcal{B}_+ (\mathcal{A}_+ \mathcal{B}_+ - \mathcal{A}_- \mathcal{B}_-)} \right] |\beta|^2 \right\} \\ &\times I_0 \left[\frac{8(1-u) U_{rs} V_{pq} |\beta|^2}{\mathcal{A}_+ \mathcal{B}_+ - \mathcal{A}_- \mathcal{B}_-} \right], \end{aligned}$$

with

$$\begin{aligned}
\mathfrak{C}_{pq}^{rs}(x, y; t) &= [xA_y + (1-u)y]^{-1} \left\{ A_y U_{rs}^2 + 2(1-u) \cos \left[\frac{\pi(r+s-p-q)}{2^{\ell+1}} \right] U_{rs} V_{pq} + A_x V_{pq}^2 \right\}, \\
\mathfrak{D}_{pq}^{rs}(x, y; t) &= \cos \left[\frac{\pi(r-s)}{2^{\ell+1}} \right] U_{rs} + \cos \left[\frac{\pi(p-q)}{2^{\ell+1}} \right] V_{pq}, \\
U_{rs}(x) &= \cos \left[\frac{\pi(r-s)}{2^{\ell+1}} \right] x + i \sin \left[\frac{\pi(r-s)}{2^{\ell+1}} \right], \\
V_{pq}(y) &= \cos \left[\frac{\pi(p-q)}{2^{\ell+1}} \right] y + i \sin \left[\frac{\pi(p-q)}{2^{\ell+1}} \right], \\
A_{rs}(t) &= \cos \left[\frac{\pi(r-s)}{2^{\ell+1}} \right] (1-u) - i \sin \left[\frac{\pi(r-s)}{2^{\ell+1}} \right] [1 + (1+2\bar{n})u], \\
B_{pq}(t) &= \cos \left[\frac{\pi(p-q)}{2^{\ell+1}} \right] (1-u) - i \sin \left[\frac{\pi(p-q)}{2^{\ell+1}} \right] [1 + (1+2\bar{n})u], \\
\mathcal{A}_{\pm}(x; t) &= [1 \pm (1+2\bar{n})u]x \pm (1-u), \\
\mathcal{B}_{\pm}(y; t) &= [1 \pm (1+2\bar{n})u]y \pm (1-u), \\
A_x(t) &= 2(1+2\bar{n})ux + (1-u), \\
A_y(t) &= 2(1+2\bar{n})uy + (1-u).
\end{aligned}$$

Furthermore, the phonon distribution function is given by

$$P_{nm}^{(\ell)}(t) = 2|N_n^{(2^{\ell+1})}|^2 \frac{(-1)^{n+m}}{n!} \frac{\partial^n}{\partial x^n} \frac{\mathcal{A}_-^m x^n}{\mathcal{A}_+^{m+1}} I_m(x; t) \Big|_{x=1}, \quad (\text{A13})$$

where

$$I_m(x; t) = \sum_{r,s=1}^{2^{\ell+1}} \exp \left(-\frac{2A_{rs}U_{rs}|\beta|^2}{\mathcal{A}_+} \right) L_m \left[\frac{4(1-u)U_{rs}^2|\beta|^2}{\mathcal{A}_+\mathcal{A}_-} \right].$$

It is important mentioning that Eqs. (A11)-(A13) were calculated by means of the parametric representation for the associated Laguerre polynomial [52], i.e.,

$$L_n^{(\alpha)}(z) = e^z \frac{1}{n!} \frac{d^n}{dx^n} x^{n+\alpha} e^{-xz} \Big|_{x=1}.$$

The total and diagonal purities determined in this appendix corroborate that obtained by Souza Silva et al. [16] for $n = 0$.

-
- [1] V.V. Dodonov, ‘Nonclassical’ states in quantum optics: a ‘squeezed’ review of the first 75 years, J. Opt. B: Quantum Semiclass. Opt. 4 (2002) R1, and references therein.
 - [2] C. Monroe, D.M. Meekhof, B.E. King, D.J. Wineland, A ‘Schrodinger cat’ superposition state of an atom, Science 272 (1996) 1131.
 - [3] D.M. Meekhof, C. Monroe, B.E. King, W.M. Itano, D.J. Wineland, Generation of nonclassical motional states of a trapped atom, Phys. Rev. Lett. 76 (1996) 1796.
 - [4] D. Leibfried, D.M. Meekhof, B.E. King, C. Monroe, W.M. Itano, D.J. Wineland, Experimental determination of the motional quantum state of a trapped atom, Phys. Rev. Lett. 77 (1996) 4281.
 - [5] W.M. Itano, C. Monroe, D.M. Meekhof, D. Leibfried, B.E. King, D.J. Wineland, Quantum harmonic oscillator state synthesis and analysis, SPIE Proc. 2995 (1997) 43.
 - [6] R.L. de Matos Filho, W. Vogel, Nonlinear coherent states, Phys. Rev. A 54 (1996) 4560.
 - [7] S.A. Gardiner, J.I. Cirac, P. Zoller, Nonclassical states and measurement of general motional observables of a trapped ion, Phys. Rev. A 55 (1997) 1683.
 - [8] C.C. Gerry, Generation of Schrodinger cats and entangled coherent states in the motion of a trapped ion by a dispersive interaction, Phys. Rev. A 55 (1997) 2478.

- [9] S.-B. Zheng, G.-C. Guo, Generation of superpositions of coherent states of the motion of a trapped ion, *Eur. Phys. J. D* 1 (1998) 105.
- [10] H. Moya-Cessa, S. Wallentowitz, W. Vogel, Quantum-state engineering of a trapped ion by coherent-state superpositions, *Phys. Rev. A* 59 (1999) 2920.
- [11] W.D. José, S.S. Mizrahi, Generation of circular states and Fock states in a trapped ion, *J. Opt. B: Quantum Semiclass. Opt.* 2 (2000) 306.
- [12] V. Man'ko, G. Marmo, A. Porzio, S. Solimeno, F. Zaccaria, Trapped ions in laser fields: A benchmark for deformed quantum oscillators, *Phys. Rev. A* 62 (2000) 053407.
- [13] G. Huyet, S. Franke-Arnold, S.M. Barnett, Superposition states at finite temperature, *Phys. Rev. A* 63 (2001) 043812.
- [14] Z. Kis, W. Vogel, L. Davidovich, Nonlinear coherent states of trapped-atom motion, *Phys. Rev. A* 64 (2001) 033401.
- [15] M. Feng, Preparation of Schrödinger cat states with cold ions beyond the Lamb-Dicke limit, *Phys. Lett. A* 282 (2001) 230.
- [16] A.L.S. Silva, W.D. José, V.V. Dodonov, S.S. Mizrahi, Production of two-Fock states superpositions from even circular states and their decoherence, *Phys. Lett. A* 282 (2001) 235.
- [17] S.-B. Zheng, Preparation of arbitrary finite superpositions of Fock states for the center-of-mass motion of two trapped ions, *J. Opt. B: Quantum Semiclass. Opt.* 3 (2001) 328.
- [18] F.L. Semião, A. Vidiella-Barranco, J.A. Roversi, Nonclassical effects in cold trapped ions inside a cavity, *Phys. Rev. A* 66 (2002) 063403.
- [19] N.B. An, T.M. Duc, Generation of three-mode nonclassical vibrational states of ions, *Phys. Rev. A* 66 (2002) 065401.
- [20] S. Schneider, G.J. Milburn, Decoherence in ion traps due to laser intensity and phase fluctuations, *Phys. Rev. A* 57 (1998) 3748.
- [21] R.M. Serra, N.G. de Almeida, W.B. da Costa, M.H.Y. Moussa, Decoherence in trapped ions due to polarization of the residual background gas, *Phys. Rev. A* 64 (2001) 033419.
- [22] A.A. Budini, R.L. de Matos Filho, N. Zagury, Decoherence in non-classical states of a trapped ion, *J. Opt. B: Quantum Semiclass. Opt.* 4 (2002) S462.
- [23] A.A. Budini, R.L. de Matos Filho, N. Zagury, Localization and dispersivelike decoherence in vibronic states of a trapped ion, *Phys. Rev. A* 65 (2002) 041402(R).
- [24] J.F. Poyatos, J.I. Cirac, P. Zoller, Quantum reservoir engineering with laser cooled trapped ions, *Phys. Rev. Lett.* 77 (1996) 4728.
- [25] Q.A. Turchette, C.J. Myatt, B.E. King, C.A. Sackett, D. Kielpinski, W.M. Itano, C. Monroe, D.J. Wineland, Decoherence and decay of motional quantum states of a trapped atom coupled to engineered reservoirs, *Phys. Rev. A* 62 (2000) 053807; C.J. Myatt, B.E. King, Q.A. Turchette, C.A. Sackett, D. Kielpinski, W.M. Itano, C. Monroe, D.J. Wineland, Decoherence of quantum superpositions through coupling to engineered reservoirs, *Nature* 403 (2000) 269; Q.A. Turchette, D. Kielpinski, B.E. King, D. Leibfried, D.M. Meekhof, C.J. Myatt, M.A. Rowe, C.A. Sackett, C.S. Wood, W.M. Itano, C. Monroe, D.J. Wineland, Heating of trapped ion from the quantum ground state, *Phys. Rev. A* 61 (2000) 063418.
- [26] J.I. Cirac, P. Zoller, Quantum computations with cold trapped ions, *Phys. Rev. Lett.* 74 (1995) 4091.
- [27] C. Monroe, D.M. Meekhof, B.E. King, W.M. Itano, D.J. Wineland, Demonstration of a fundamental quantum logic gate, *Phys. Rev. Lett.* 75 (1995) 4714.
- [28] D. Jonathan, M.B. Plenio, P.L. Knight, Fast quantum gates for cold trapped ions, *Phys. Rev. A* 62 (2000) 042307, and references therein.
- [29] D. Kielpinski, A. Ben-Kish, J. Britton, V. Meyer, M.A. Rowe, C.A. Sackett, W.M. Itano, C. Monroe, D.J. Wineland, Recent results in trapped-ion quantum computing at NIST, [quant-ph/0102086](https://arxiv.org/abs/quant-ph/0102086), 2001.
- [30] D. Jonathan, M.B. Plenio, Light-shift-induced quantum gates for ions in thermal motion, [quant-ph/0103140](https://arxiv.org/abs/quant-ph/0103140), 2001.
- [31] M. Feng, X. Wang, Implementation of quantum gates and preparation of entangled states in cavity QED with cold trapped ions, [quant-ph/0112031](https://arxiv.org/abs/quant-ph/0112031) v2, 2002.
- [32] M. Feng, Quantum computing with trapped ions in an optical cavity via Raman transition, *Phys. Rev. A* 66 (2002) 054303.
- [33] D.J. Wineland, M. Barret, J. Britton, J. Chiaverini, B. DeMarco, W.M. Itano, B. Jelenković, C. Langer, D. Leibfried, V. Meyer, T. Rosenband, T. Schätz, Quantum information processing with trapped ions, [quant-ph/0212079](https://arxiv.org/abs/quant-ph/0212079) v1, 2002, and references therein.
- [34] M.A. Marchiolli, L.F. da Silva, P.S. Melo, C.M.A. Dantas, Quantum-interference effects on the superposition of N displaced number states, *Physica A* 291 (2001) 449.
- [35] S. Wallentowitz, W. Vogel, Reconstruction of the Quantum Mechanical State of a Trapped Ion, *Phys. Rev. Lett.* 75 (1995) 2932.
- [36] V.V. Dodonov, S.S. Mizrahi, A.L.S. Silva, Decoherence and thermalization dynamics of a quantum oscillator, *J. Opt. B: Quantum Semiclass. Opt.* 2 (2000) 271.
- [37] J. Plebański, Classical properties of oscillator wave packets, *Bull. Acad. Pol. Sci.* 2 (1954) 213.
- [38] F.A.M. de Oliveira, P.L. Knight, V. Bužek, Properties of displaced number states, *Phys. Rev. A* 41 (1990) 2645.
- [39] C. Monroe, D.M. Meekhof, B.E. King, S.R. Jefferts, W.M. Itano, D.J. Wineland, Resolved-Sideband Raman Cooling of a Bound Atom to the 3D Zero-Point Energy, *Phys. Rev. Lett.* 75 (1995) 4011.
- [40] C.A. Sackett, D. Kielpinski, B.E. King, C. Langer, V. Meyer, C.J. Myatt, M. Rowe, Q.A. Turchette, W.M. Itano, D.J. Wineland, C. Monroe, Experimental entanglement of four particles, *Nature* 404 (2000) 256.
- [41] R.L. de Matos Filho, W. Vogel, Quantum Nondemolition Measurement of the Motional Energy of a Trapped Atom, *Phys. Rev. Lett.* 76 (1996) 4520.
- [42] D.J. Wineland, C. Monroe, W.M. Itano, D. Leibfried, B.E. King, D.M. Meekhof, Experimental Issues in Coherent Quantum-

State Manipulation of Trapped Atomic Ions, *J. Res. Natl. Inst. Stand. Technol.* 103 (1998) 259.

- [43] D. Leibfried, R. Blatt, C. Monroe, D. Wineland, Quantum dynamics of single trapped ions, *Rev. Mod. Phys.* 75 (2003) 281.
- [44] L. Davidovich, M. Orszag, N. Zagury, Quantum nondemolition measurements of vibrational populations in ionic traps, *Phys. Rev. A* 54 (1996) 5118.
- [45] H.J. Carmichael, *Statistical Methods in Quantum Optics 1: Master Equations and Fokker-Planck Equations*, Springer, Berlin, 1999.
- [46] S. Chountasis, A. Vourdas, Weyl functions and their use in the study of quantum interference, *Phys. Rev. A* 58 (1998) 848.
- [47] S. Chountasis, A. Vourdas, Weyl and Wigner functions in an extended phase-space formalism, *Phys. Rev. A* 58 (1998) 1794.
- [48] Recently, Turchette et al. [25] have investigated motional heating of laser-cooled ${}^9\text{Be}^+$ ions held in radio-frequency (Paul) traps, and measured heating rates in a variety of traps with different geometries, electrode materials, and characteristic sizes. This important experiment has shown that “the magnitude of heating rates of the size-scaling measurements are inconsistent with thermal electronic noise as the source of the heating.”
- [49] A.I. Lvovsky, S.A. Babichev, Synthesis and tomographic characterization of the displaced Fock state of light, *Phys. Rev. A* 66 (2002) 011801(R).
- [50] G.N. Watson, *A treatise on the theory of Bessel functions*, Cambridge University Press, New York, 1996.
- [51] N.N. Lebedev, *Special Functions and Their Applications*, Dover, New York, 1972.
- [52] A.W. Niukkanen, Clebsch-Gordan-type linearisation relations for the products of Laguerre polynomials and hydrogen-like functions, *J. Phys. A: Math. Gen.* 18 (1985) 1399.